Electronic Supplementary Material (ESI) for Polymer Chemistry.

Supporting Information

Antibacterial and Cytotoxic Properties of Star-shaped Quaternary Ammonium-functionalized Polymers with Different Pendant Groups

So Young Nam,[a] Jaesung Lee,[a] Seung Su Shin,[a] Hyun Jung Yoo,[b] Myeongji Yun,[a] Seohyun Kim,[b] Ji Hyung Kim*[b] and Jung-Hyun Lee*[a]

[a] *Department of Chemical and Biological Engineering, Korea University, 145 Anam-ro, Seongbuk-gu, Seoul 02841, Republic of Korea. E-mail: leejhyyy@korea.ac.kr*

[b] *Department of Biotechnology, Korea University, 145 Anam-ro, Seongbuk-gu, Seoul 02841, Republic of Korea. E-mail: jay_kim@korea.ac.kr*

S1. Synthesis of L-QAR

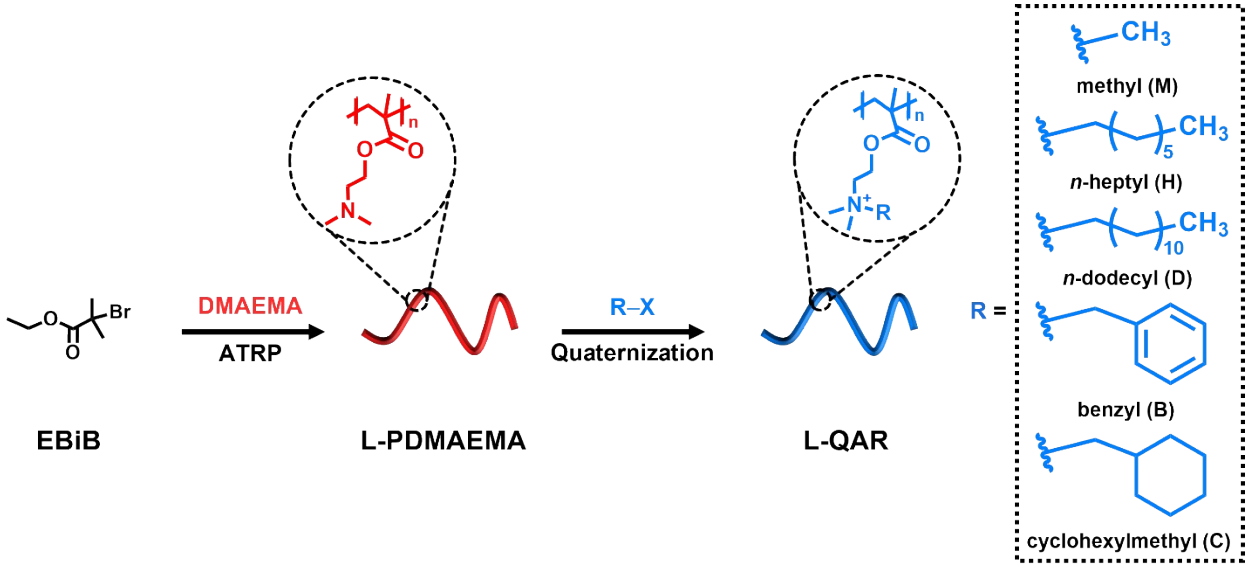

Fig. S1 Schematic synthesis of linear quaternary ammonium polymers (L-QARs) containing various pendant groups (R)–methyl (M), *n*-heptyl (H), *n*-dodecyl (D), benzyl (B), and cyclohexylmethyl (C).

S2. Chemical analysis of CD-Br

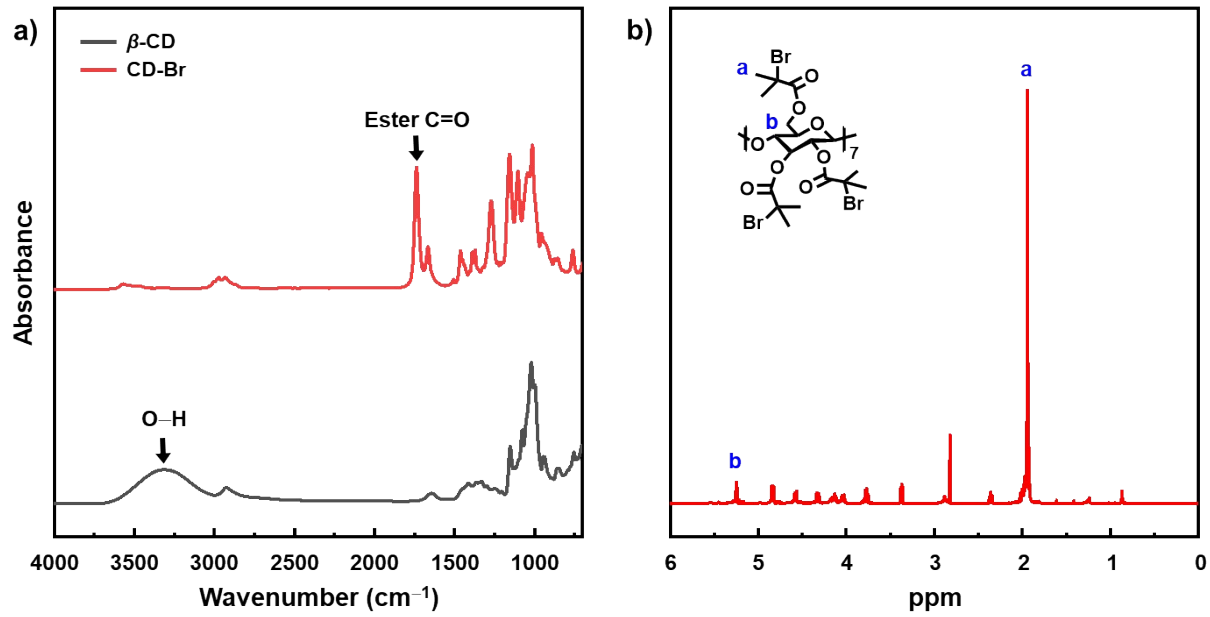

Fig. S2 (a) FT-IR spectra of β-CD and CD-Br. The disappearance of the hydroxyl group peak at 3,350 cm^{-1} and appearance of a new ester group peak at 1,728 cm^{-1} for CD-Br confirmed the successful functionalization of β-CD with BiBB initiators via esterification. (b) ^{1}H NMR spectra of CD-Br. The degree of substitution (E) of the hydroxyl groups of β-CD to BiBB was calculated to be ~90% (*i.e.,* ~19 of 21 hydroxyl groups of β-CD was substituted with BiBB) by the following equation: $E = A_a/18A_b \times 100$, where A_a and A_b are the integral areas of the peaks corresponding to a and b protons, respectively, in the ^{1}H NMR spectra.[1]

CD-Br: ^{1}H NMR (500 MHz, $CDCl_3$) δ 1.92 (a, C(Br)–$(CH_3)_2$, 6H), 5.25 (b, O–CH–C, 1H)

S3. Characterization of L-PDMAEMA and S-PDMAEMA

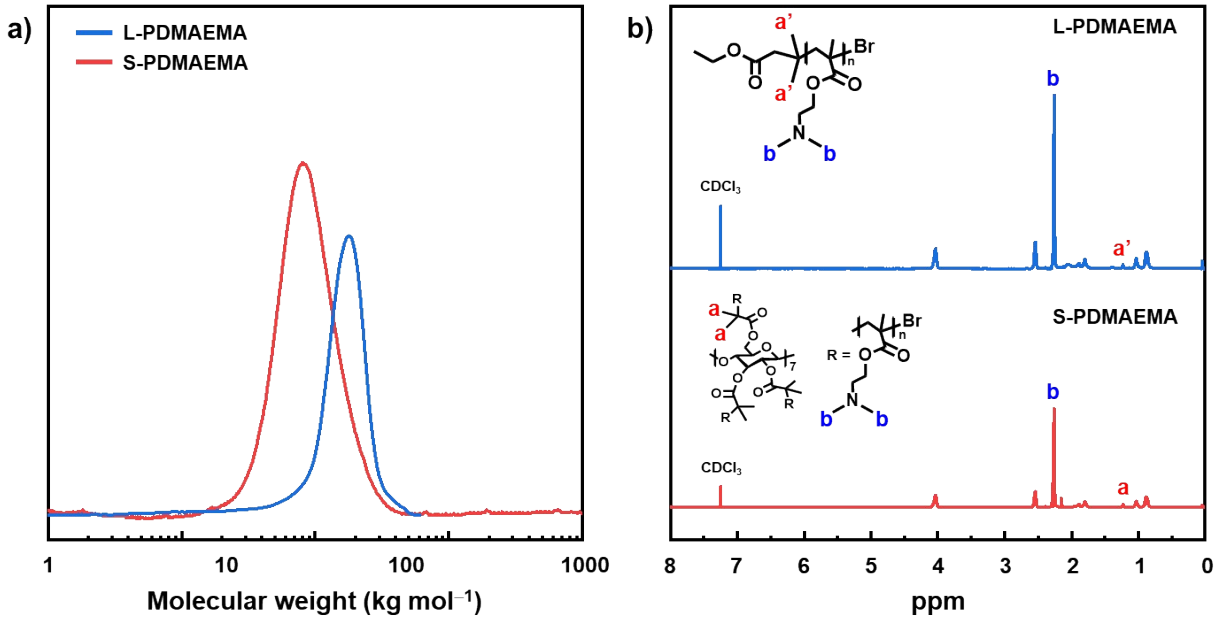

c)

Polymer	Relative M_w[a] (kg mol^{-1})	Absolute M_w[b] (kg mol^{-1})	M_w/M_n[c]
L-PDMAEMA	188.5	183.1	1.11
S-PDMAEMA	92.3	185.2	1.06

Fig. S3 (a) GPC spectra, (b) ^{1}H NMR spectra, and (c) molecular weight of L-PDMAEMA and S-PDMAEMA. The total number of the DMAEMA repeating units of L-PDMAEMA (N_L) and S-PDMAEMA (N_s) was calculated by $N_L = A_b/A_{a'}$ and $Ns = 19A_b/A_a$, respectively, where A_a, $A_{a'}$, and A_b are the integral areas of the peaks corresponding to a, a' and b protons, respectively.[1] The total M_w of L-PDMAEMA ($M_{w,L}$) and S-PDMAEMA ($M_{w,S}$) was calculated by multiplying N_L and N_S, respectively, by the M_w value (=157.21 g mol^{-1}) of DMAEMA as follows: $M_{w,L} = 157.21 \times N_L$ and $M_{w,S} = 157.21 \times N_S$.[1]

L-PDMAEMA: ^{1}H NMR (500 MHz, $CDCl_3$) δ1.12 (a', C–CH_3, 3H), 2.2 (b, N–$(CH_3)_2$, 6H)

S-PDMAEMA: ^{1}H NMR (500 MHz, $CDCl_3$) δ1.12 (a, C–CH_3, 3H), 2.2 (b, N–$(CH_3)_2$, 6H)

S4. Chemical analysis of S-QARs

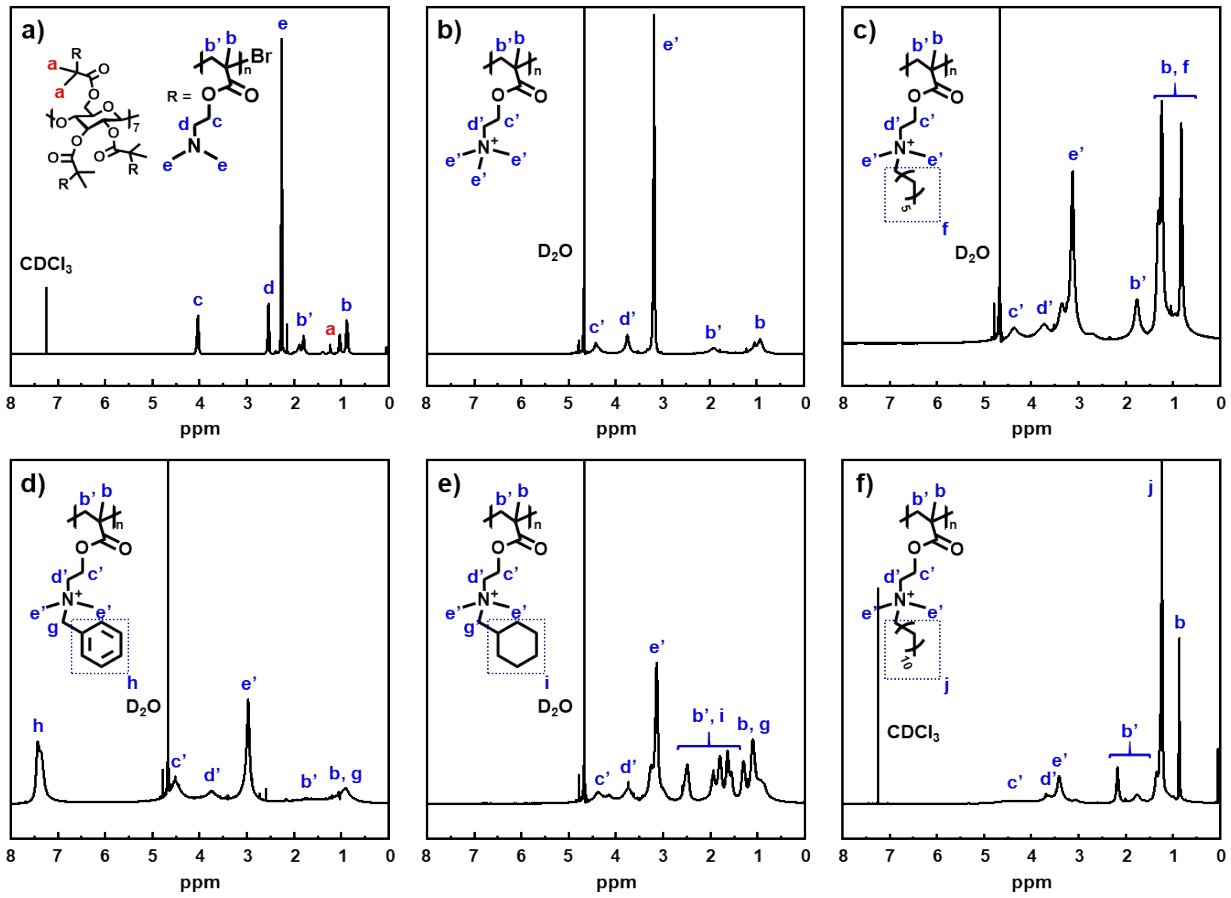

Fig. S4 ^{1}H NMR spectra of the star-shaped polymers before and after quaternization. (a) S-PDMAEMA, (b) S-QAM, (c) S-QAH, (d) S-QAB, (e) S-QAC, and (f) S-QAD.[2,3] Because the number of the repeating units of the S-PDMAEMA and S-QAR polymers is identical, the total M_w of S-QAR was calculated by multiplying the number of its repeating units by the M_w value of its repeating unit.

(a) S-PDMAEMA: ^{1}H NMR (500 MHz, $CDCl_3$) δ1.12 (a', C–CH_3, 3H), 0.81–1.10 (b, C–CH_3, 3H), 1.86 (b', C–CH_2–C, 2H), 4.07 (c, O–CH_2–C, 2H), 2.65 (d, C–CH_2–N, 2H), 2.2 (e, N–$(CH_3)_2$, 6H)

(b) S-QAM: ^{1}H NMR (500 MHz, D_2O) δ0.81–1.10 (b, C–CH_3, 3H), 1.86 (b', C–CH_2–C, 2H), 4.45 (c', O–CH_2–C, 3H), 3.8 (d', C–CH_2–N^+, 2H), 3.10-3.30 (e', N^+–$(CH_3)_3$, 9H)

(c) S-QAH: ^{1}H NMR (500 MHz, D_2O) δ0.81–1.10 (b, C–CH_3, 3H), 1.86 (b', C-CH_2-C, 2H), 4.45 (c', O–CH_2–C, 2H), 3.8 (d', C–CH_2–N^+, 2H), 2.91–3.40 (e', N^+–$(CH_3)_2$, 6H), 1.13–1.54 (f, N^+–$(CH_2)_6$–CH_3, 15H)

(d) S-QAB: ^{1}H NMR (500 MHz, D_2O) δ0.81-1.10 (b, C–CH_3, 3H), 1.86 (b', C–CH_2–C, 2H), 4.56 (c', O–CH_2–C, 2H), 3.8 (d', C–CH_2–N^+, 2H), 2.82–3.38 (e', N^+–$(CH_3)_2$, 6H), 0.8–1.13 (g, N^+–CH_2–C, 2H), 7.4-7.7 (h, C–$(CH)_5$, 5H)

(e) S-QAC: ^{1}H NMR (500 MHz, D_2O) δ 0.81–1.10 (b, C–CH_3, 3H), 1.86 (b', C–CH_2–C, 2H), 4.45 (c', O–CH_2–C, 2H), 3.8 (d', C–CH_2–N^+, 2H), 2.82–3.28 (e', N^+–$(CH_3)_2$, 6H), 0.8–1.13 (g, N^+-CH_2-C, 2H), 1.48–2.56 (i, C-CH–$(CH_2)_5$ 11H)

(f) S-QAD: ^{1}H NMR (500 MHz, D_2O) δ 0.81–1.10 (b, C–CH_3, 3H), 1.86 (b', C–CH_2–C, 2H), 4.45 (c', O–CH_2–C, 2H), 3.8 (d', C–CH_2–N^+, 2H), 3.12–3.45 (e', N^+–$(CH_3)_2$, 6H), 1.13–1.54 (j, N^+–$(CH_2)_{11}$–CH_3, 25H)

S5. Chemical analysis of L-QARs

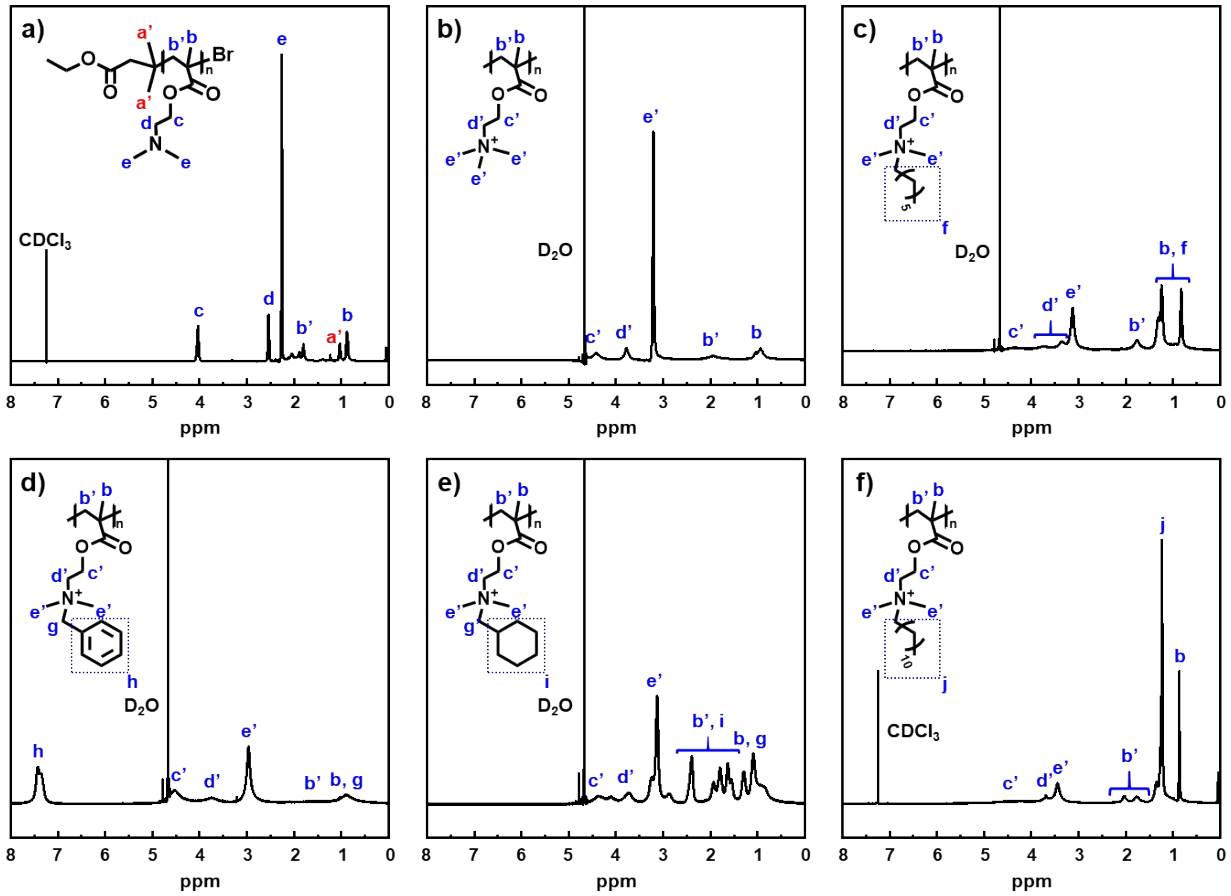

Fig. S5 ^{1}H NMR spectra of the linear polymers before and after quaternization. (a) L-PDMAEMA, (b) L-QAM, (c) L-QAH, (d) L-QAB, (e) L-QAC, and (f) L-QAD.[2,3] Because the number of the repeating units of the L-PDMAEMA and L-QAR polymers is identical, the total M_w of L-QAR was calculated by multiplying the number of its repeating units by the M_w value of its repeating unit.

(a) L-PDMAEMA: ^{1}H NMR (500 MHz, $CDCl_3$) δ1.12 (a', C–CH_3, 3H), 0.81–1.10 (b, C–CH_3, 3H), 1.86 (b', C–CH_2–C, 2H), 4.07 (c, O–CH_2–C, 2H), 2.65 (d, C–CH_2–N, 2H), 2.2 (e, N–$(CH_3)_2$, 6H)

(b) L-QAM: ^{1}H NMR (500 MHz, D_2O) δ0.81–1.10 (b, C–CH_3, 3H), 1.86 (b', C–CH_2–C, 2H), 4.45 (c', O–CH_2–C, 3H), 3.8 (d', C–CH_2–N^+, 2H), 3.10–3.30 (e', N^+–$(CH_3)_3$, 9H)

(c) L-QAH: ^{1}H NMR (500 MHz, D_2O) δ0.81–1.10 (b, C–CH_3, 3H), 1.86 (b', C–CH_2–C, 2H), 4.45 (c', O–CH_2–C, 2H), 3.8 (d', C–CH_2–N^+, 2H), 2.91–3.40 (e', N^+–$(CH_3)_2$, 6H), 1.13-1.54 (f, N^+–$(CH_2)_6$–CH_3, 15H)

(d) L-QAB: ^{1}H NMR (500 MHz, D_2O) δ0.81–1.10 (b, C–CH_3, 3H), 1.86 (b', C–CH_2–C, 2H), 4.56 (c', O-CH_2–C, 2H), 3.8 (d', C–CH_2–N^+, 2H), 2.82–3.38 (e', N^+–$(CH_3)_2$, 6H), 0.8–1.13 (g, N^+–CH_2–C, 2H), 7.4–7.7 (h, C–$(CH)_5$, 5H)

(e) L-QAC: ^{1}H NMR (500 MHz, D_2O) δ 0.81–1.10 (b, C–CH_3, 3H), 1.86 (b', C–CH_2–C, 2H), 4.45 (c', O–CH_2–C, 2H), 3.8 (d', C–CH_2–N^+, 2H), 2.82–3.28 (e', N^+–$(CH_3)_2$, 6H), 0.8-1.13 (g, N^+–CH_2–C, 2H), 1.48–2.56 (i, C–CH–$(CH_2)_5$ 11H)

(f) L-QAD: ^{1}H NMR (500 MHz, D_2O) δ 0.81–1.10 (b, C–CH_3, 3H), 1.86 (b', C–CH_2–C, 2H), 4.45 (c', O–CH_2–C, 2H), 3.8 (d', C–CH_2–N^+, 2H), 3.12–3.45 (e', N^+–$(CH_3)_2$, 6H), 1.13–1.54 (j, N^+–$(CH_2)_{11}$–CH_3, 25H)

S6. Chemical analysis of the polymers

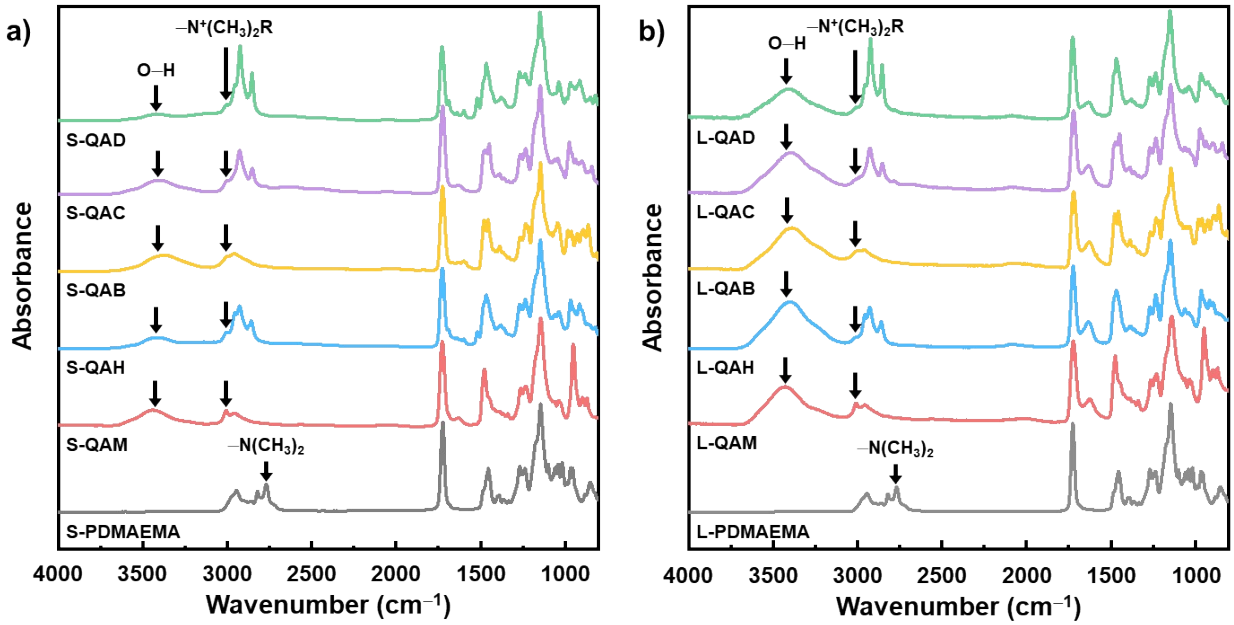

Fig. S6 FT-IR spectra of (a) star-shaped and (b) linear polymers before and after quaternization. After quaternization of PDMAEMA, its characteristic peak of the tertiary amine group ($–N(CH_3)_2$) at 2,769 cm^{-1} completely disappeared, while the new peaks of the hydroxyl (O–H) and QA group ($–N^+ (CH_3)_2R$) at 3,430 and 3,020 cm^{-1}, respectively, appeared.[4,5] This result confirms that the tertiary amine groups of S-/L-PDMAEMA were completely converted into QA groups via quaternization to form S-/L-QARs.

S7. Water solubility of the polymers

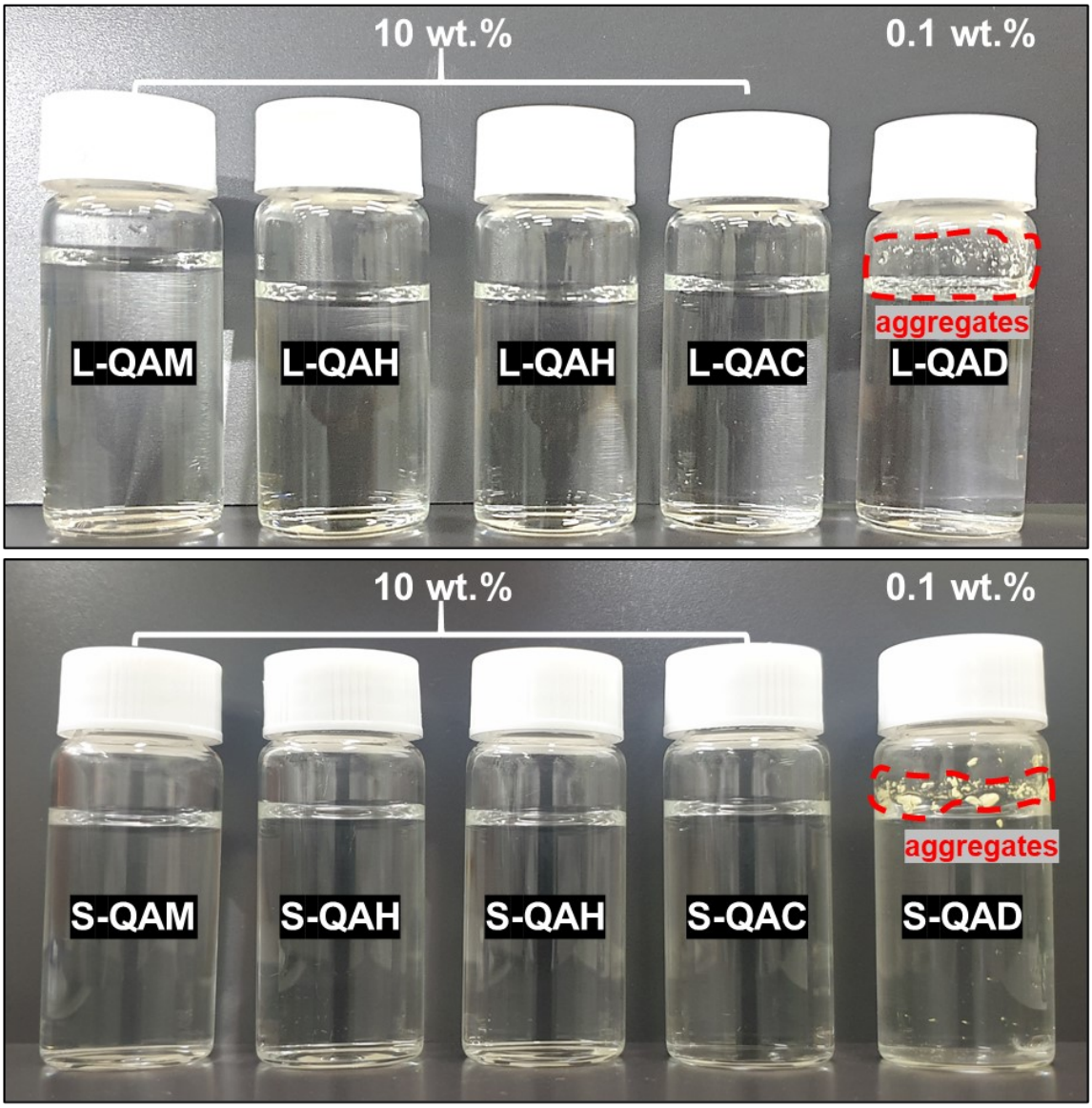

Fig. S7 Photographs of the polymer solutions in DI water of (a) L-QARs and (b) S-QARs. While the QAD polymers (even at 0.1 wt.%) were not completely dissolved in water with causing significant aggregation (denoted by dotted red lines), the other polymers were well dissolved in water even at high concentrations (>10 wt.%).

S8. Water contact angle of the polymer films

To prepare a series of polymer films, the syntheised polymer was was dissolved in an ethanol (50 vol.%) aqueous solution to prepare a polymer (1 wt.%) solution, which was then uniformly spread on a cleaned silicon wafer, followed by oven drying at 60 °C for 24 h. The water contact angles of the prepared polymer films were measured using a contact angle goniometer (Phoenix-300, SEO Corporation), as summarized in Table S1. The hydrophobicity of the polymer estimated by its water contact angle decreased depending on its pendant group in the order of QAD >> QAH > QAC >> QAB ≈ QAM, which is consistent with the analysis by log *P*.

Polymer	Water contact angle (°)				
	QAM	QAH	QAB	QAC	QAD
L-QAR	15.3 ± 0.4	61.3 ± 0.7	15.1 ± 0.5	48.9 ± 0.8	98.4 ± 4.5
S-QAR	15.3 ± 0.5	59.6 ± 0.9	14.7 ± 0.7	46.9 ± 0.2	95.4 ± 1.1

Table S1. Water contact angles of the polymer films prepared via drop coating.

S9. Antibacterial activity and toxicity of the polymers

Table S2. MBC, HC_{50}, and IC_{50} (in mass concentration units) of the synthesized QA polymers.

Polymer	MBC (μg mL^{-1})		Cell toxicity (μg mL^{-1})	
	S. aureus	*E. coli*	HC_{50}	IC_{50}
L-QAM	>871.3	>871.3	>871.3	67.1
L-QAH	5.9	11.7	<7.6	32.3
L-QAB	7.3	955.3	>955.3	81.2
L-QAC	4.7	7.8	>972.8	60.3
L-QAD	>1,182.8	>1,182.8	201.9	–
L-QAM	>874.5	>874.5	>874.5	56.8
S-QAH	3.0	5.9	<7.7	45.3
S-QAB	4.2	964.8	>964.8	83.9
S-QAC	2.4	4.9	>979.5	62.7
S-QAD	>1,191.5	1,191.5	104.0	–

S10. Effect of the counterion type on the antibacterial activity of the QAM polymers

The iodide counterion of the L-QAM and S-QAM polymers was exchanged with the bromide ion as follows. The QAM polymer aqueous solution in a dialysis tube (MWCO: 10 kg mol^{-1}) was immersed in a NaBr (1 M) aqueous solution for 5 days and then DI water for 5 days. The complete conversion of the iodide counterion to bromide was confirmed by the XPS analysis of the QAM polymers before and after the ion exchange process as shown in Table S3.

Table S3. XPS atomic ratio relative to the N atomic content of the QAM polyemrs before and after ion exchange.

Polymer		L-QAM		S-QAM	
Ion exchage		Before	After	Before	After
Atomic ratio	N	1	1	1	1
	I	0.84	0.01	0.86	<0.01
	Br	–	0.80	–	0.83

Next, the antibacterial activity of L-QAM and S-QAM with bromide counterions (L-QAM-Br and S-QAM-Br) against *S. aureus* and *E. coli* was assessed using the MIC and MBC assay and compared with their counterparts with iodide counterions (L-QAM and S-QAM) (Table S4). No noticeable difference in the antibacterial activity of the QAM polymers with different counterions demonstrated the negligible effect of the counterion type on their antibacterial activity.

Table S4. MIC and MBC of L-QAM and S-QAM with different counterions.

	S. aureus			*E. coli*		
	In LB broth		In PBS	In LB broth		In PBS
	MIC (nM)	MBC (nM)	MBC (nM)	MIC (nM)	MBC (nM)	MBC (nM)
L-QAM-Br	500	500	>2,500	1,250	>2,500	>2,500
L-QAM	500	500	>2,500	1,250	>2,500	>2,500
S-QAM-Br	312.5	312.5	>2,500	1,000	>2,500	>2,500
S-QAM	312.5	312.5	>2,500	1,000	>2,500	>2,500

S11. Antibacterial activity of the polymers in LB broth

The antibacterial activity of the polymers in LB was evaluated by determining their minimum inhibitory concentration (MIC) and MBC against *S. aureus* and *E. coli* based on the standard broth microdilution method[6] and colony counting method,[7] respectively. A polymer (5,000 nM) stock solution was prepared in a DMSO (10 vol.%)/PBS aqueous solution and then sequentially diluted up to 10 nM. Bacteria were grown in a LB solution at 37 °C for 24 h. The bacterial solution (0.1 mL) was diluted in a fresh LB solution (5 mL) and cultivated for 2 h, followed by bacteria separation via centrifugation at 7,000 rpm for 10 min. Collected bacteria were resuspended in a fresh LB solution and diluted to ~1×10^6 CFU mL^{-1}. The prepared bacterial suspension (50 μL) was mixed with the polymer solution at each concentration (50 μL) in a 96-well round-bottom microplate and incubated at 37 °C for 19 h. MIC was determined by the lowest polymer concentration, at which no bacterial growth was observed with naked eye. The bacteria-polymer solution (10 μL) was pipetted onto a LB agar plate, streaked, and incubated at 37 °C overnight to determine MBC, at which no colony unit was observed in the LB agar plate. The tests were repeated three times with duplicate samples for all the polymers. A bacteria solution in DMSO (5 vol.%)/LB without the polymer was used as a positive control, while a DMSO (5 vol.%)/LB solution without the polymer was used as a negative control.

S12. Antibacterial activity of the polymers in LB broth

Table S5. MIC and MBC (in molar concentration units) of the polymers in LB broth.

Polymer	*S. aureus*		*E. coli*	
	MIC (nM)	MBC (nM)	MIC (nM)	MBC (nM)
L-QAM	500	500	1,250	>2,500
L-QAH	750	1,000	625	625
L-QAB	1,250	1,250	750	1,000
L-QAC	625	625	500	500
L-QAD	>2,500	>2,500	>2,500	>2,500
S-QAM	312.5	312.2	1,000	>2,500
S-QAH	375	375	312.5	312.5
S-QAB	500	500	500	500
S-QAC	250	250	250	312.5
S-QAD	>2,500	>2,500	>2,500	>2,500

S13. Antibacterial activity of the polymers in LB broth

Table S6. MIC and MBC (in mass concentration units) of the polymers in LB broth.

Polymer	*S. aureus*		*E. coli*	
	MIC (μg mL^{-1})	MBC (μg mL^{-1})	MIC (μg mL^{-1})	MBC (μg mL^{-1})
L-QAM	174.3	174.3	435.6	>871.2
L-QAH	293.7	391.6	244.8	244.8
L-QAB	477.6	477.6	286.6	382.1
L-QAC	243.2	243.2	194.6	194.6
L-QAD	>1182.8	>1182.8	>1182.8	>1182.8
L-QAM	109.3	109.3	349.8	>874.5
S-QAH	147.8	147.8	123.2	123.2
S-QAB	193.0	193.0	193.0	193.0
S-QAC	98.0	98.0	98.0	122.4
S-QAD	>1191.5	>1191.5	>1191.5	>1191.5

S14. Size of the polymers in LB

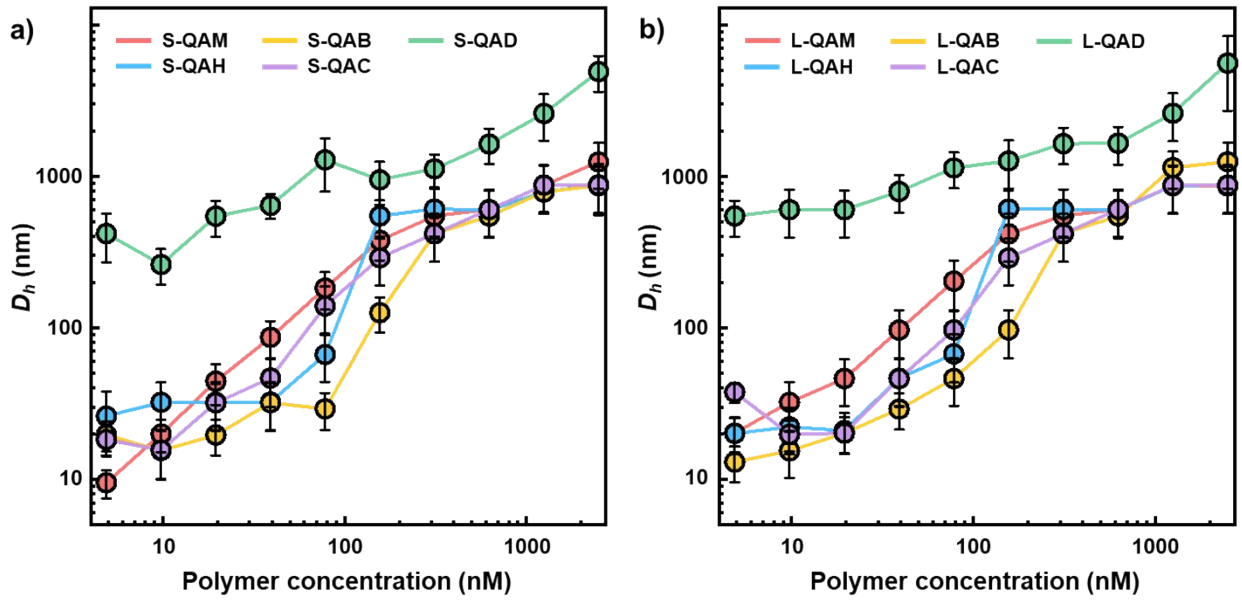

Fig. S8 Hydrodynamic diameter (D_h) of (a) S-QARs and (b) L-QARs in the LB medium used for the MIC/MBC assay as a function of the polymer concentration. The polymer size increases with increasing the polymer concentration, and its tendency depends on the pendant group structure.

S15. Size and charge of the polymers

Table S7. Hydrodynamic diameter (D_h), zeta potential, and charge density of the polymers in the LB medium.

Polymer	D_h (nm)	Zeta potential (mV)	Charge density ($\times 10^{-9}$ mV nm^{-3})
L-QAM	864.7 ± 290.7	4.7 ± 0.5	13.9
L-QAH	874.3 ± 309.5	−1.0 ± 0.8	−2.8
L-QAB	1247.5 ± 419.3	1.0 ± 0.5	1.0
L-QAC	872.8 ± 307.7	2.2 ± 0.7	6.3
L-QAD	5586.6 ± 2873.2	13.1 ± 2.9	0.1
S-QAM	1247.2 ± 418.8	12.4 ± 0.4	12.2
S-QAH	879.8 ± 323.7	−1.4 ± 0.6	−3.9
S-QAB	868.0 ± 297.0	0.3 ± 0.5	0.9
S-QAC	873.2 ± 307.7	4.3 ± 1.2	12.3
S-QAD	4914.9 ± 1307.9	−28.0 ± 0.8	−0.5

S16. Hemolysis assay of the polymers

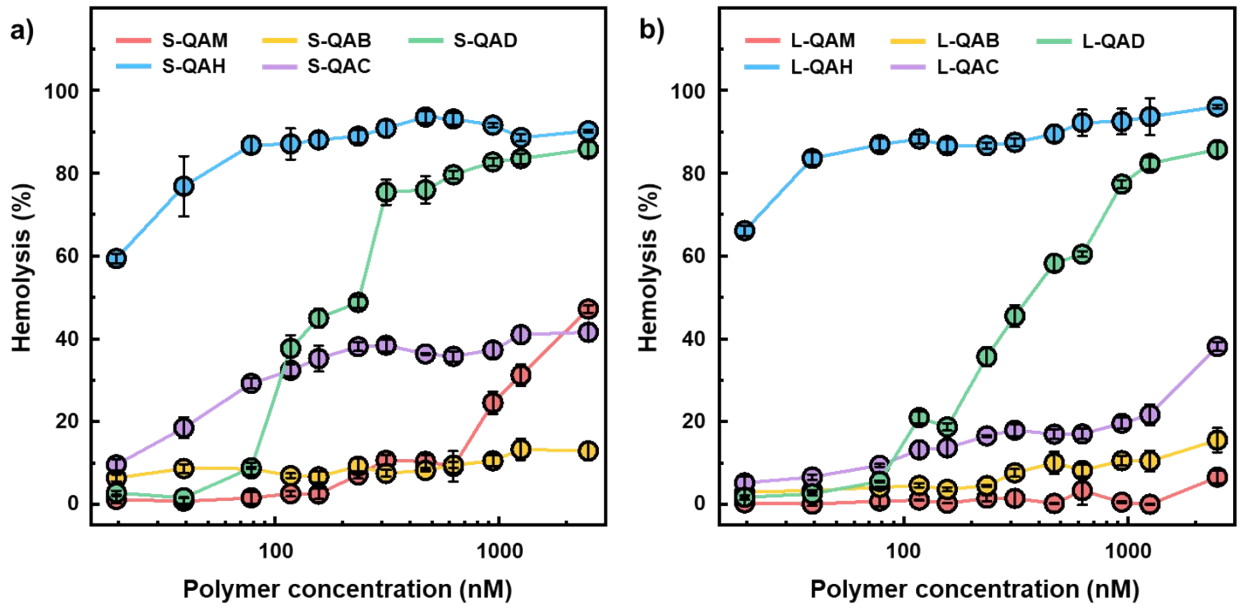

Fig. S9 Hemolytic activity of (a) S-QARs and (b) L-QARs as a function of the polymer concentration.

S17. Hemolysis assay of S-QARs

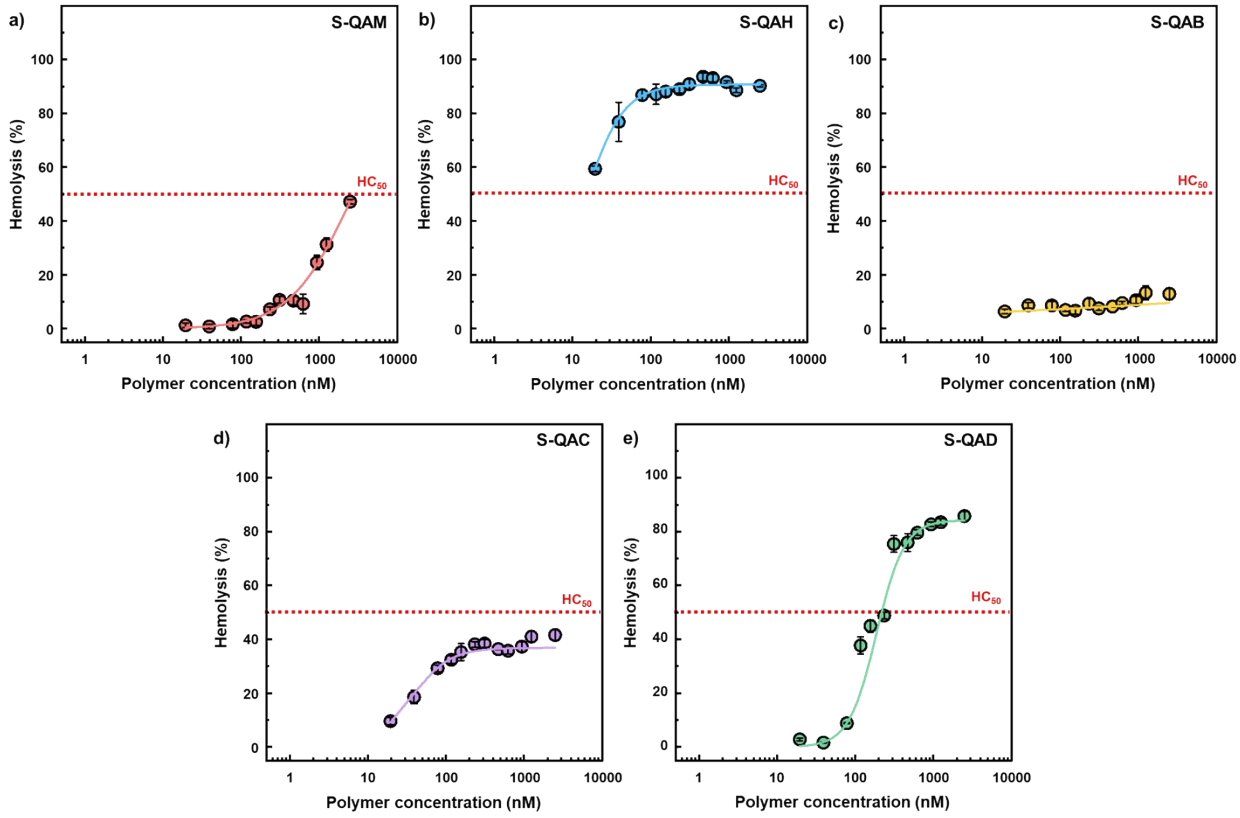

Fig. S10 Fitting of hemolysis experimental results to the Hill equation of (a) S-QAM, (b) S-QAH, (c) S-QAB, (d) S-QAC, and (e) S-QAD. The dotted red line denotes HC_{50} that induces 50% hemolysis.

S18. Hemolysis assay of L-QARs

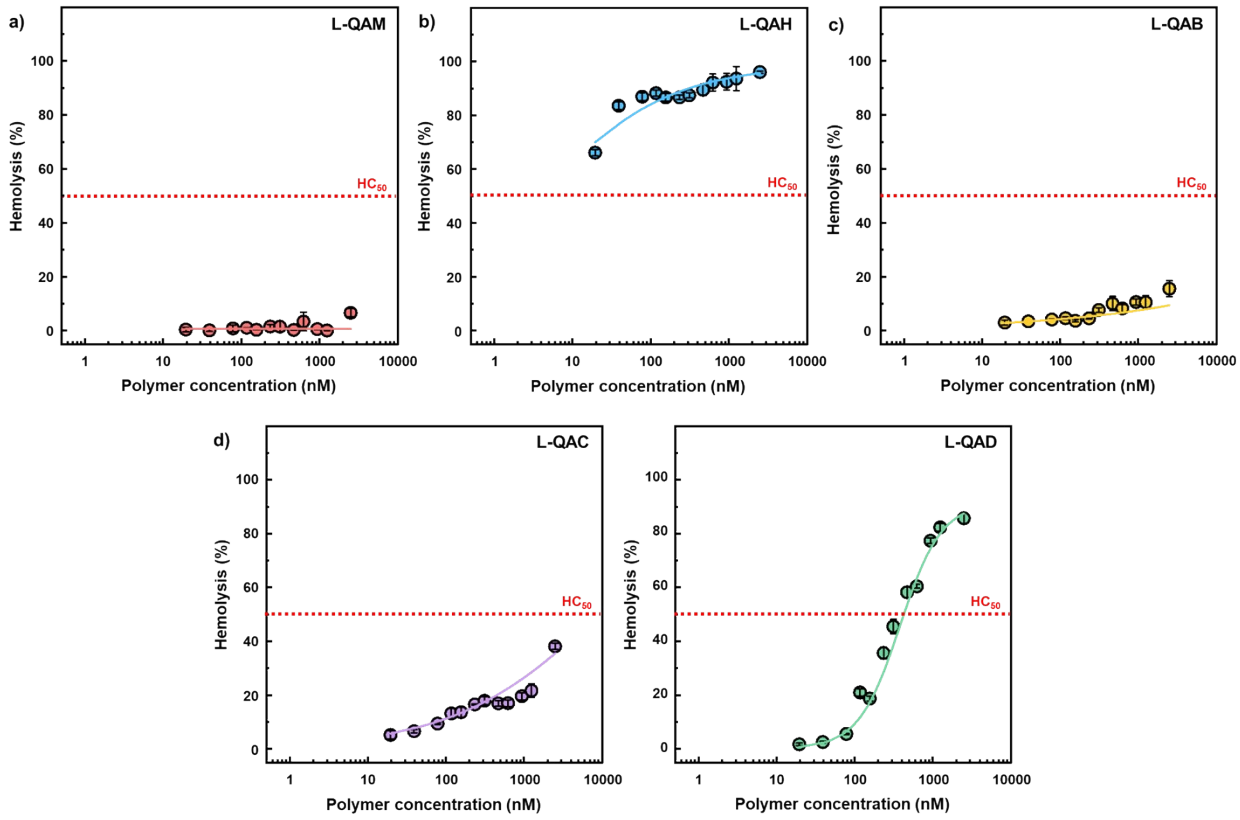

Fig. S11 Fitting of hemolysis experimental results to the Hill equation of (a) L-QAM, (b) L-QAH, (c) L-QAB, (d) L-QAC, and (e) L-QAD. The dotted red line denotes HC_{50} that induces 50% hemolysis.

S19. MTT assay of the polymers

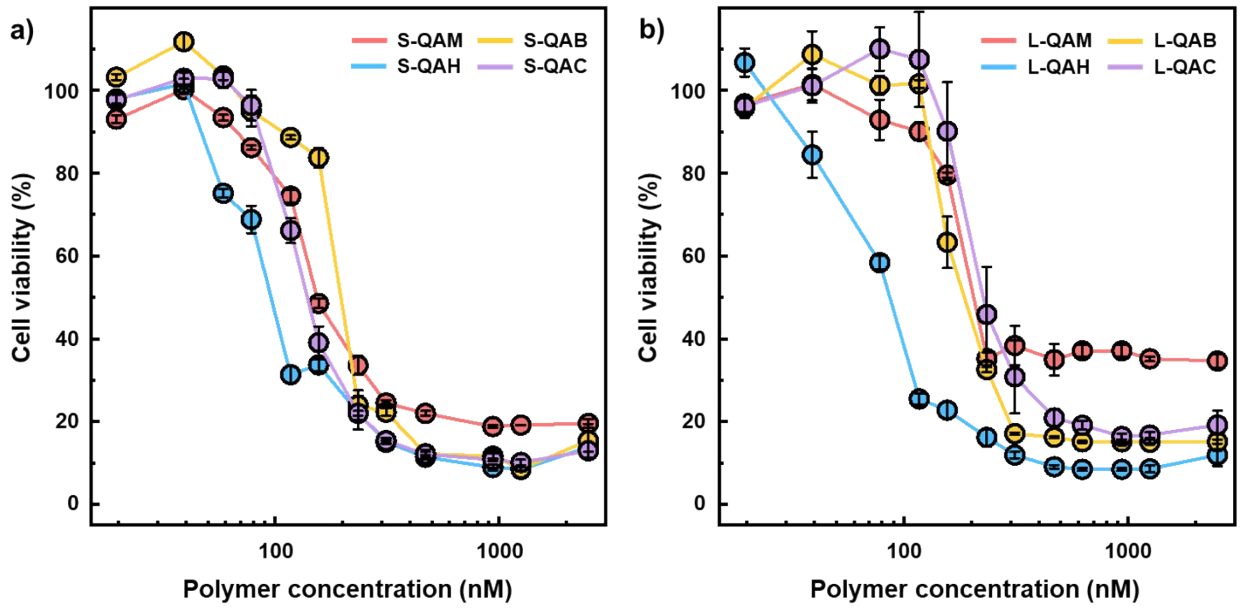

Fig. S12 Cell viability of A549 cells treated with (a) S-QARs and (b) L-QARs as a function of the polymer concentration.

S20. MTT assay of S-QARs

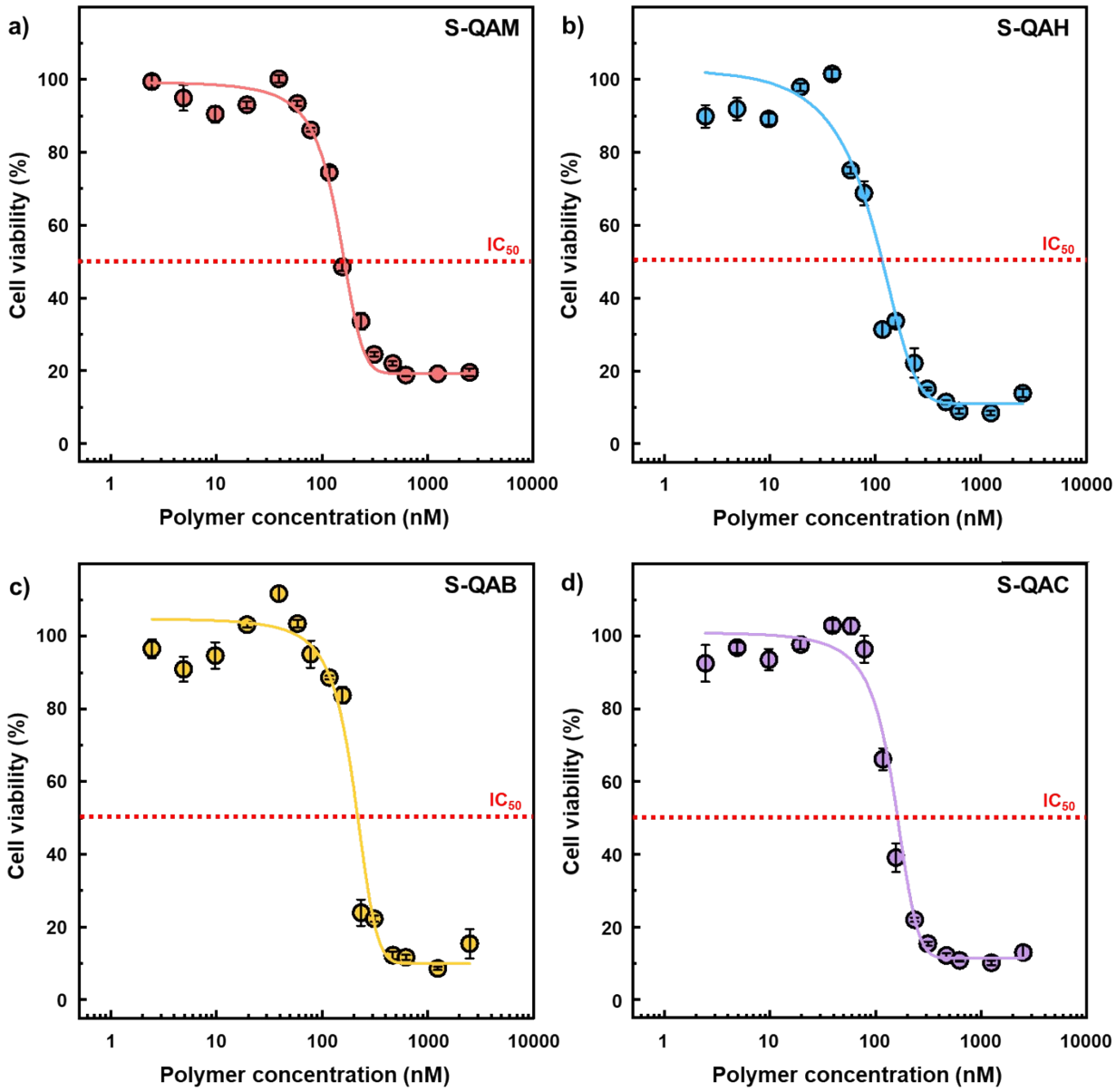

Fig. S13 Fitting of cell viability experimental results to the dose-response curve of (a) S-QAM, (b) S-QAH, (c) S-QAB, and (d) S-QAC. The dotted red line denotes IC_{50} that induces 50% cell death.

S21. MTT assay of L-QARs

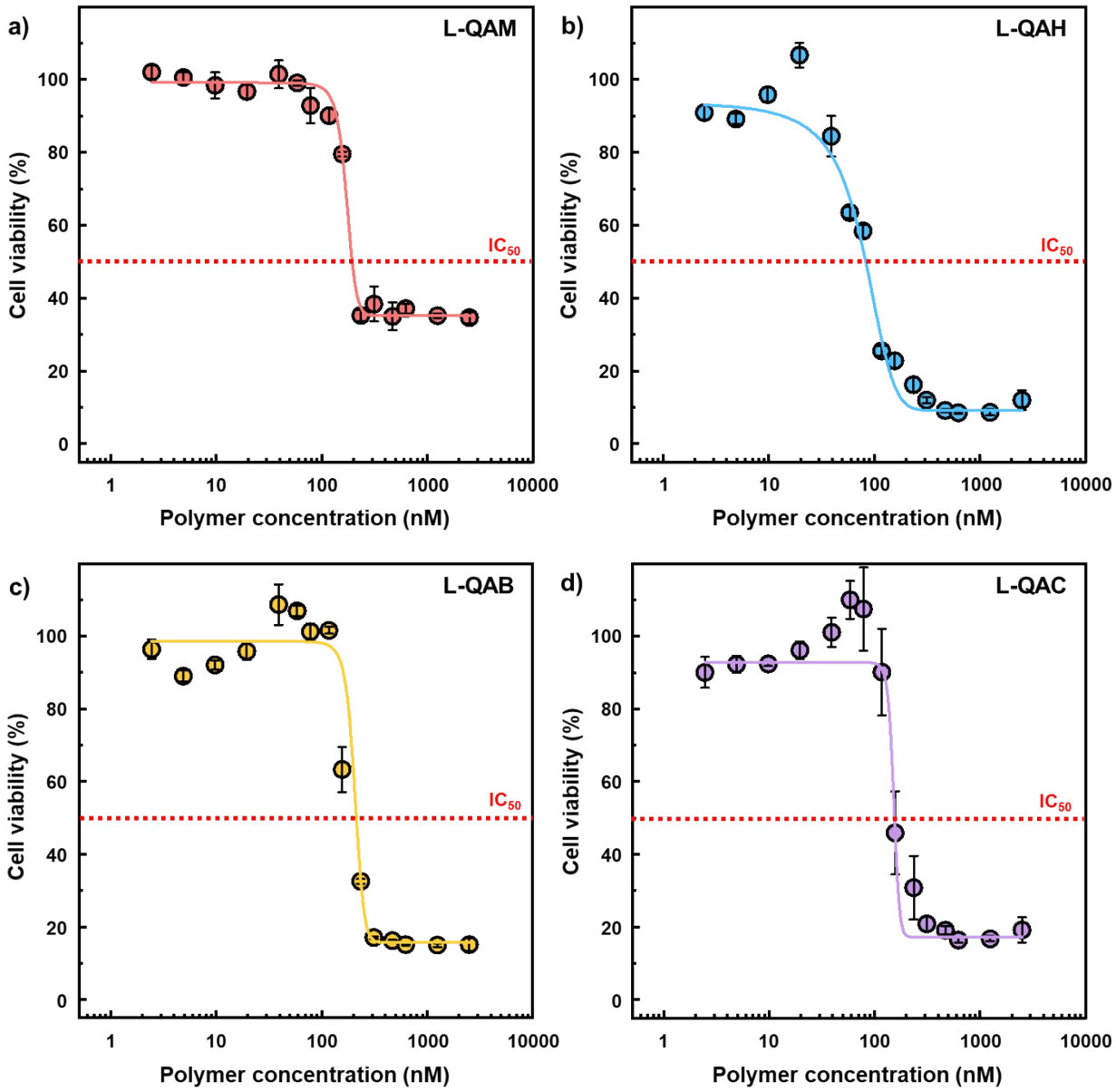

Fig. S14 Fitting of cell viability experimental results to the dose-response curve of (a) L-QAM, (b) L-QAH, (c) L-QAB, and (d) L-QAC. The dotted red line denotes IC_{50} that induces 50% cell death.

References

1 F. J. Xu, Z. X. Zhang, Y. Ping, J. Li, E. T. Kang, K. G. Neoh, *Biomacromolecules,* 2009, **10**, 285–293.

2 G. Lu, D. Wu, R. Fu, *React. Funct. Polym.,* 2007, **67**, 355–366.

3 J.-A. Park, K. Y. Cho, C. H. Han, A. Nam, J.-H. Kim, S.-H. Lee, J.-W. Choi, *Sci. Rep.,* 2019, **9**, 383.

4 J.-J. Yin, F. Wahid, Q. Zhang, Y.-C. Tao, C. Zhong, L.-Q. Chu, *Macromol. Mater. Eng.,* 2017, **306**, 1700069.

5 V. Chrysostomou, S. Pispas, *J. Polym. Sci., Part A: Polym. Chem.,* 2017, **56**, 598–610.

6 M. Álvarez-Paino, A. Muñoz-Bonilla, F. López-Fabal, J. L. Gómez-Garcés, J. P. A. Heuts, M. Fernández-García, *Biomacromolecules,* 2015, **16**, 295–303.

7 S.-J. Richards, K. Isufi, L. E. Wilkins, J. Lipecki, E. Fullam, M. I. Gibson, *Biomacromolecules,* 2018, **19**, 256–264.